Recyclable, Biobased Photoresins for 3D Printing through Dynamic Imine Exchange

Karen P. Cortés-Guzmán,[1] Ankit R. Parikh,[2] Marissa L. Sparacin,[1] Ashele K. Remy,[1] Lauren Adegoke,[4] Chandani Chitrakar,[4] Melanie Ecker,[4] Walter E. Voit,[2,3] Ronald A. Smaldone*[1,3]

[1]Department of Chemistry and Biochemistry, University of Texas at Dallas, 800 West Campbell Road, Richardson, Texas 75080, United States

[2]Department of Mechanical Engineering UT Dallas University of Texas at Dallas, 800 West Campbell Road, Richardson, Texas 75080, United States

[3]Department of Materials Science and Engineering UT Dallas University of Texas at Dallas, 800 West Campbell Road, Richardson, Texas 75080, United States

[4]Department of Biomedical Engineering, University of North Texas, 1155 Union Circle #310440, Denton, Texas 75203, United States

Abstract

Transimination reactions are highly effective dynamic covalent reactions to enable reprocessability in thermosets, as they can undergo exchange without the need for catalysts, by exposing the materials to external stimuli such as heat. In this work, a series of five biobased vanillin derived resin formulations consisting of vanillin acrylate with vanillin methacrylate functionalized Jeffamines® were synthesized, and 3D printed using digital light projection (DLP). The resulting thermosets produced, displayed a range of mechanical properties (Young's modulus 2.05 – 332 MPa) which allow for an array of applications. The materials we obtained have self-healing abilities which were characterized by scratch healing tests. Additionally, dynamic transimination reactions enable these thermosets to be reprocessed when thermally treated above their glass transition temperatures under high pressures using a hot-press. Due to the simple synthetic procedures and the readily available commercial Jeffamines®, these materials will aid in promoting a shift to materials with predominantly biobased content and help drift away from polymers made from non-renewable resources.

Keywords: Vanillin, vitrimer, biobased thermoset, 3D Printing, dynamic covalent chemistry, covalent adaptable networks, imine, self-healing, thermally reprocessable, photocuring

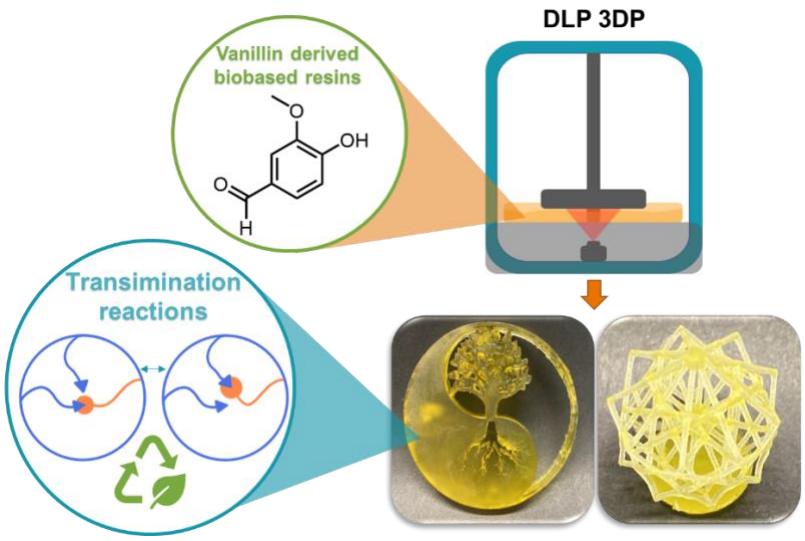

Introduction

Polymeric materials, or plastics, combine unrivalled mechanical properties with low cost, and have become a staple commodity of our modern lifestyles. However, while offering many advantages, the new plastics economy still has major weaknesses that are becoming more evident by the day. Plastics are mainly produced from fossil fuels –a non-renewable resource– with a major carbon footprint that will become much more impactful as the population and demand increase.[1] Furthermore, environmental pollution caused by plastics is creating broad devastation in natural ecosystems and is considered one of the greatest environmental challenges of our time.[2] Based on this, the design of new polymeric materials should be mindful of sustainability practices that consider the process "*from cradle to grave*". Starting materials should be obtained from renewable feedstocks to reduce the carbon footprint from their production.[3] Vanillin is a biobased, aromatic compound derived from lignin that is widely used as a flavor and fragrance ingredient. However, most industrially produced vanillin is still obtained from petroleum-based sources as it represents a cheaper alternative. Sustainable vanillin production still accounts for a very small portion of the world's supply, but it is expected to continue to grow in the coming years, based on its promise as a potential substitute of petroleum derived monomers like bisphenol A (BPA)[4] and styrene.[5] It is anticipated that the sustainable production of vanillin-derived phenolics will be encouraged in large scale as new markets are developed for its application.[6]

In addition to using renewable resources, once the useful life of the material is over, it is important to provide alternative methods for disposal, such as composting and recycling, to prevent them from ending up in landfills. Recycling is a high-value mechanism to repurpose plastics at the end of their life, ideally, into materials for applications of similar quality. The recycling pathway is desirable for most uses since this keeps the material in the economy, reducing the need for additional production.[7] Additionally, the ability to repair high value polymers or objects can extend their

lifetimes, resulting in a reduction of single use plastics. Many examples of self-healing polymers have been produced where covalent bonds can be reformed using a catalyst[8,9] or reconfigured through dynamic covalent exchange reactions.[10–12]

On the other hand, new materials that are compatible with competitive manufacturing methods, such as three-dimensional printing (3DP), are essential 3DP –the process of transforming computer-based designs into 3D structures– is achieved through layer-by-layer deposition or polymerization of a material.[13] The advantages, such as sustainability,[14] low waste production,[15] and customizability[16] have made this a popular technique, which is projected to augment or replace other common manufacturing methods like injection molding in the future.[17] Among 3D printing technologies, vat photopolymerization (VP) methods like stereolithography (SLA) and digital light projection (DLP), provide the highest resolution products and can provide isotropic materials, which are key to obtaining optimal mechanical performance. VP methods produce thermoset polymers, which contain covalent crosslinks between the polymer chains, and cannot be recycled by melt processing. In recent years, this limitation has been addressed through the development of covalent adaptable networks (CANs),[18–21] and the number of CANs that use VP is rapidly growing. CANs incorporate dynamic functionalities that can be broken and reformed upon exposure to external stimuli, while in some cases, maintaining their overall bond density.[22] CANs are now bridging the gap between thermoplastics and thermosets, enabling thermosets to have the recycling and reprocessing advantages of thermoplastics.

A few biobased CANs have been reported, usually consisting of associative bond exchange mechanisms, which are known as vitrimers.[23–26] Although a minority, there are some reports of 3D printed materials that take advantage of CANs, with direct ink writing (DIW) being the most used technique.[27,28] Nonetheless, a few reports that combine the use of VP and CANs have been documented.[29] There have been a few examples of self-healing polymers used in 3D printing so far,[30–33] but only a handful are compatible with VP.[34–37]

Most of the reports available combining CANs and VP use transesterification reactions.[38] However, among other areas of dynamic covalent chemistry, imine exchange reactions have numerous advantages.[39,40] They can occur rapidly and without any significant side reactions, there are a wide variety of structures available, simple synthetic approaches, and they have a diverse range of applications.[41,42] Several reports utilizing these chemistries exist, however, they are used mainly to develop materials for extrudable hydrogels,[43] epoxy resins,[44,45] elastomers,[46] or seldomly, methacrylate resins, which have not been 3D printed. Xu *et al*,[47] reported two biobased, thermally reprocessable, and chemically recyclable imine vitrimers based on methacrylate resins. The use of methacrylates (rather than acrylates) with amine groups can help to avoid aza-Michael side reactions.[48] However, methacrylate containing resins can have reduced printability due to slower photopolymerization kinetics[29] or high viscosities which can compromise their

compatibility with photo-based 3D printers.[47] Here, we report a series of five obased, self-healable, and reprocessable resinformulations that consist of an optimized mixture of vanillin methacrylate-functionalized Jeffamines®, and vanillin acrylate. The addition of vanillin acrylate allows for a reduction of the viscosity while providing sufficiently rapid photopolymerization kinetics to allow it to be successfully printed with a DLP 3D printer – without compromising the amount of bio-based content in the photoresin formulation. Additionally, the presence of imine moieties allow for the self-healing and reprocessing capabilities.

Experimental Section

Materials

All chemicals were used as received unless otherwise noted. Vanillin (99%) was purchased from Alfa Aesar. Triethylamine (TEA), sodium chloride (NaCl) sodium bicarbonate ($NaHCO_3$), hydrochloric acid (HCl), sodium hydroxide (NaOH), dichloromethane (DCM), and tetrahydrofuran (THF) were purchased from Fisher Scientific. Acryloyl chloride (≥97% stabilized with phenothiazine) was purchased from Sigma-Aldrich. 4-dimethylaminopyridine (99%) (DMAP) was purchased from Acros Organics. Methacrylic anhydride (94% stabilized with *ca*. 0.2% 2,4-dimethyl-6-tertbutylphenol) was purchased from Alfa Aesar. Jeffamine® T-403 (J-T-403), Jeffamine® D-400 (J-D-400), Jeffamine® ED-900 (J-ED-900), Jeffamine® D-2000 (J-D-2000), and Jeffamine® T-3000 (J-T-3000) were obtained as samples from Huntsman. Diphenyl(2,4,6-trimethylbenzoyl) phosphine oxide (TPO) was purchased from TCI.

Synthetic Procedures

Vanillin Acrylate (VA). VA was synthesized following previously reported procedures.[49,50] Vanillin (40g, 0.26 mol) was added to a round bottom flask and dissolved in anhydrous DCM, followed by addition of TEA (51.4g, 0.51 mol). The mixture was purged with N_2 and cooled to 0-5°C in an ice bath. Acryloyl chloride (16.9g, 0.19mol) was added dropwise over a period of one hour. The reaction contents were stirred for 24 hours, and vacuum filtered to remove precipitates. The filtrate was then washed with water, $NaHCO_3$ (sat. aq.), HCl (0.1M, aq.), brine, and finally dried over Na_2SO_4. The product was purified using column chromatography (6:4 hexane / ethyl acetate), to obtain the product as a clear and colorless liquid (32.8g, 60%). (^{1}H NMR Figure S1)

Vanillin Methacrylate (VMA) VMA was synthesized following previously reported procedures.[47] Vanillin (20g, 0.13 mol) was added to a round bottom flask, followed by addition of DMAP (0.12g, 0.98 mmol), and methacrylic anhydride (22g, 0.14mol). The mixture was refluxed at 60°C for 24 h, then cooled to room temperature. The reaction mixture was washed with water, $NaHCO_3$ (sat. aq.), NaOH (0.5M, aq.), NaOH (1M, aq.), brine, and dried over Na_2SO_4. A white crystalline product was obtained and used without further purification. (23.5g, 80%). (^{1}H NMR Figure S2)

VMA-functionalized Jeffamines® The general procedure for the synthesis of the five Jeffamine crosslinkers was the following: VMA (2 equiv for the diamines and 3 equiv for the triamines) was added to a round bottom flask and dissolved in DCM, followed by addition of 1.2 equiv of the different Jeffamines® (J-T-403, J-D-400, J-ED-900, J-D-2000, and J-T-3000). The solution was stirred for 4h at room temperature. The crude product was washed with NaOH (1M, aq.), $NaHCO_3$ (sat. aq.), brine, and dried over Na_2SO_4. After evaporating the solvent at reduced pressures, the viscous liquids obtained were used without further purification. (^{1}H NMR Figure S3-S7)

Resin Formulation and 3D Printing

All the resin formulations were prepared using 20 mol% of the Jeffamine® crosslinker and 80 mol% of the diluent VA. These components were mixed with 2 wt.% of TPO photoinitiator and ultrasonicated for 30 min to degas the resin and avoid air bubbles while printing, as well as ensure full dissolution of the photoinitiator. After this, the resin was gently warmed with a heat gun to facilitate its flow out of the container, and poured into the vat of the Photon Zero DLP 3D printer. The printed shapes were ASTM D638 standard specimen type V, the raising speed was set to 3 mm/s and the exposure time set to 60 s. Once printed, the specimens were washed twice with isopropanol, the first to remove excess unreacted resin, and the second one while sonicating for 5 min to remove additional unreacted material. After washing, the specimens were post-cured under a 405 nm lamp for 24 h.

Fourier Transform Infrared Spectroscopy (FTIR)

Infrared spectra were obtained with an attenuated total reflection (ATR) accessory coupled to a Fourier transform infrared (FTIR) spectrometer (Cary 600 Series). All spectra were recorded in the 4000−400 cm^{-1} range with a resolution of 2 cm^{-1}, accumulating 32 scans.

Thermogravimetric Analysis (TGA). TGA of 5-10 mg samples loaded into an alumina crucible, was conducted from room temperature to 700 °C at 10°C/min, with a flow rate of 100 mL/min N_2 atmosphere using a Mettler Toledo SDT.

Tensile Testing

Uniaxial tensile testing to failure of ASTM D638 standard type V specimens was performed using an Instron 5500A testing machine with a 50 N load cell at a rate of 10 mm/min until failure.

Compression Testing

Uniaxial compression testing was performed using an Instron 6800 universal testing machine with a 50 kN load cell for 3D printed and reprocessed cylindrical compression samples (10 mm diameter x 10 mm height). The samples tested consisted of printed, annealed, and reprocessed samples. All printed samples were

post-cured for 24h in a 405 nm lamp after printing. Annealed samples were thermally treated in a 140 °C oven for 3.5h to replicate the conditions that the reprocessed samples had undergone. Reprocessed samples were compression molded in a hydraulic hot press for 3.5h at 140°C in a cylindrical mold. All compression tests of these samples were conducted at room temperature (25 °C) using a crosshead rate of 10 mm/min until specimen failure.

Dynamic Mechanical Analysis (DMA)

The dynamic mechanical properties of the vanillin-Jeffamine® thermosets were measured using a Discovery DMA 850 from TA Instruments in the tension mode. The samples were tested from -25 to 200°C, or -100 to 200°C accordingly at a frequency of 1 Hz, a 5°C/min heating rate and oscillation amplitude of 15 µm.

Self-Healing Experiments

For the self-healing experiments, a small piece of the printed specimen of each formulation was gently scratched using a razor blade. Optical microscopy images were obtained for each scratched specimen as the “before healing” pictures, and then were placed in between two glass slides, and held together with two binder clips to apply pressure. The chosen temperature for the healing experiments was 80°C as this is above the T_g of all the formulations. The samples were placed in an oven for 3h, and after this, optical microscopy images were obtained to evaluate the healing of each formulation. These tests were carried out in triplicate to ensure reproducibility.

Reprocessing

To evaluate the reprocessability of the samples, the printed specimens were ground into small pieces through mechanical grinding and then placed into a metallic mold and compressed under 1500 psi at 140°C for 3h using a Carver hydraulic press.

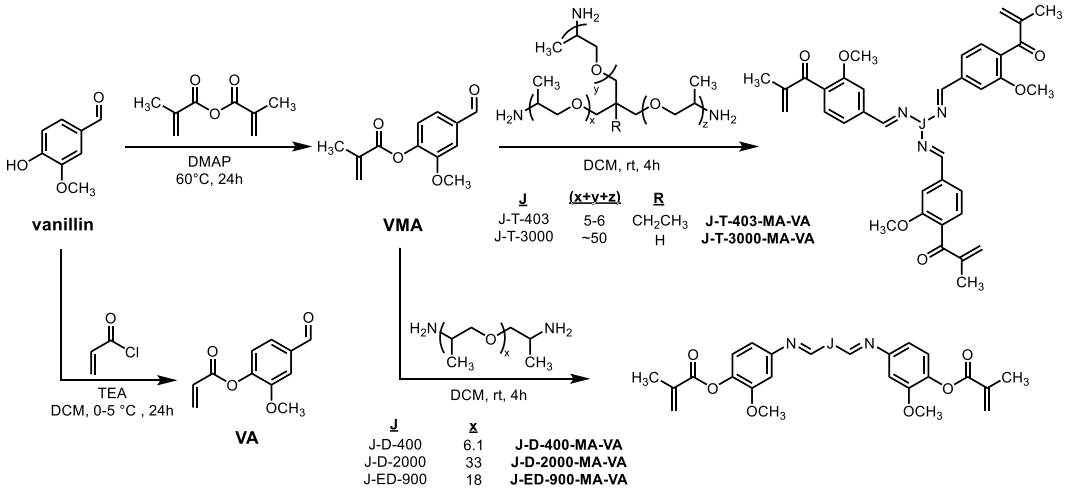

Scheme 1. General scheme for the synthesis of VA and the five different Jeffamine® crosslinkers.

Results and Discussion

Synthesis and photoreactive resin formulation for 3D printing

The synthesis of the resin components is illustrated in Scheme 1. All the resin components were functionalized with acrylate and methacrylate groups which are reactive towards radical photopolymerization. VMA was used to generate the methacrylated crosslinkers with the dynamic imine functionalities as methacrylate groups are less reactive than acrylate groups towards the aza-Michael reaction. Therefore, the Jeffamine® amine groups will predominantly react with the phenolic aldehyde group of VMA to generate the imines.

To be compatible with DLP 3D printing technologies, photoresins require low viscosity so that the resin can recoat the vat surface completely before the next printed layer. The five different imine-containing crosslinkers synthesized are all viscous liquids. To decrease this viscosity, and to retain fast enough photopolymerization kinetics for the formulation to be 3D printable, VA was used as a reactive diluent. Different formulations were created to qualitatively evaluate the printability and the best performing formulation was the 20 mol% crosslinker, and 80 mol% VA. Therefore, this composition ratio was employed for all the formulations, which showed good printing accuracy using DLP 3D printing as seen in figure 1.

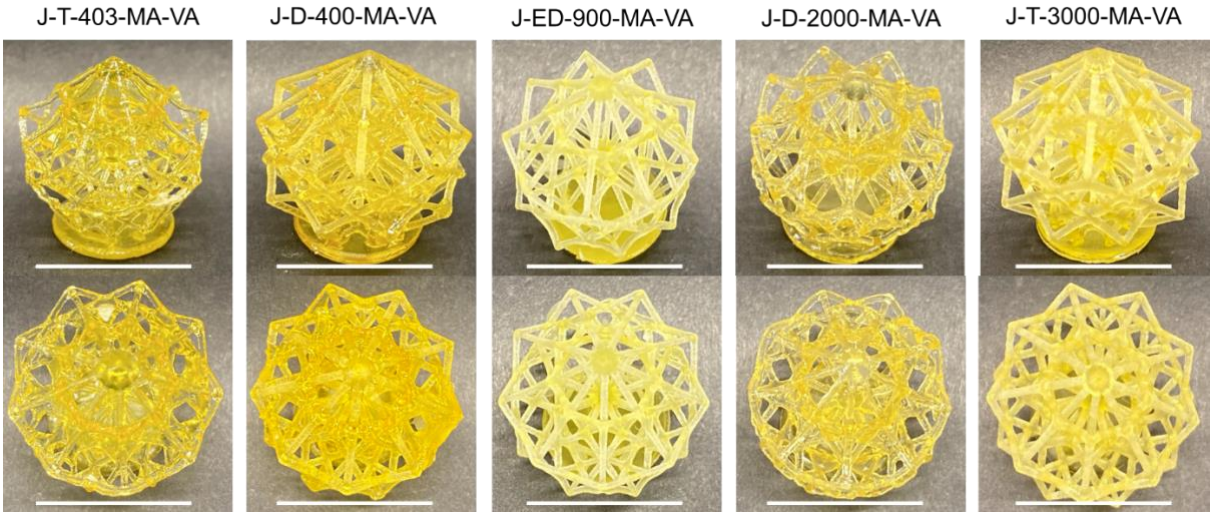

Figure 1. Complex structures printed with the five different Vanillin-Jeffamine® formulations (scale bar 2 cm).

Structural characterization

FTIR was used to confirm the presence of the imine functionalities (1645 cm^{-1}) in the cured thermosets, as well as, to evaluate the conversion of the vinyl groups by the reduction of the signal of the =C–H peak at 945 cm^{-1} (Figure S8). Additionally, gel fractions by swelling in water and ethanol, were calculated, obtaining

percentages above 95% for most of the formulations indicating good incorporation of the components into the network (Figure S9-S10).

Thermal characterization of the thermosets

TGA of the five resin formulations were obtained to evaluate their thermal stability (Figure S11). A 5 wt% decomposition temperature was observed above 150°C for all formulations indicating a max temperature range for evaluating the dynamic behaviors. DMA experiments were performed to elucidate the glass transition temperatures (T_g). Obtaining the T_g helps to determine a temperature above which the polymer networks more easily move around each other to participate in the bond rearrangement reactions. The T_g values obtained from the peak of tan δ were 66, 33, 22, -18 and -26°C for J-T-403-MA-VA, J-D-400-MA-VA, J-ED-900-MA-VA, J-D-2000-MA-VA, and J-T-3000-MA-VA respectively (Figure 2, Table 1). As a general trend we observed that the higher T_g corresponded to the lowest molecular weight tri- and diamine Jeffamines® with a polypropylene glycol backbone (J-T-403 and J-D-400). The T_g of the diamine with the polyethylene glycol backbone and intermediate molecular weight resided in the middle (J-ED-900). The lowest T_gs correspond to the di- and triamine with the highest molecular weights (J-D-2000 and J-T-3000). This can be explained by the higher imine density, as well as, the size of the chains in the crosslinker backbones. The longer the chains in the crosslinker, the lower the impediment for the rearrangement of the atoms that need to perform the exchange, resulting in lower T_gs. Additionally, the shape of the Tan δ can help us elucidate the homogeneity of the polymer networks. As seen for J-D-2000-MA-VA we observe a very broad Tan δ peak which suggests heterogeneous networks.

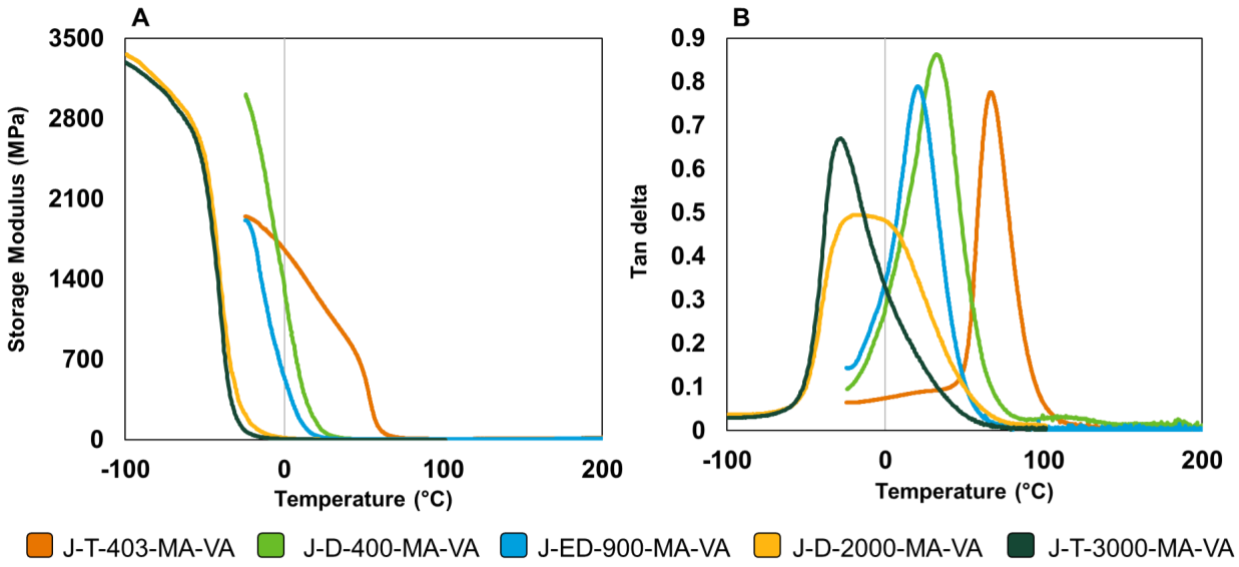

Figure 2. A) Plot of the storage modulus in MPa of the five formulations. B) Plot of the Tan delta of the five formulations.

Table 1. Dynamic Mechanical Analysis of the five formulations

Sample	Tan δ	T_g (°C)	E' at 25 °C (MPa)	E" at 25 °C (MPa)
J-T-403-MA-VA	0.71 ± 0.092	65.58 ± 1.63	1497.44 ± 470.89	147.77 ± 60.43
J-D-400-MA-VA	0.89 ± 0.031	32.99 ± 0.91	85.41 ± 13.74	64.054 ± 8.89
J-ED-900-MA-VA	0.81 ± 0.040	22.097 ± 1.82	24.53 ± 4.40	19.18 ± 4.25
J-D-2000-MA-VA	0.46 ± 0.026	-18.14 ± 6.74	3.29 ± 1.05	0.90 ± 0.31
J-T-3000-MA-VA	0.50 ± 0.16	-26.51 ± 2.94	3.90 ± 0.60	0.46 ± 0.096

T_g = Glass transition temperature (°C), E'= Storage modulus (MPa), E" = Loss modulus (MPa)

Evaluation of Mechanical Properties

Tensile testing was conducted to evaluate the mechanical properties of all the printed formulations. For each formulation, at least five specimens were tested and representative stress-strain curves of all the formulations are shown in Figure 3, as well as a comparison of the calculated ultimate tensile strength (UTS), strain at break, and Young's modulus. From the results, we observed that the J-T-403-MA-VA thermoset showed the highest UTS and Young's modulus since J-T-403 is a triamine which provides the final product with a highly crosslinked network. When compared with its equivalent diamine (in molecular weight) J-D-400-MA-VA, we observed a reduction of about half of the UTS and Young's modulus, but an increase in the strain at break. This can be explained by the fact that the crosslinking density of the diamine is lower than the triamine. This increases the UTS, but the less crosslinked polymer chains have more freedom to move around each other and relax stress which improves the elasticity. When comparing J-T-403-MA-VA and J-D-400-MA-VA with their equivalents J-T-3000-MA-VA and J-D-2000-MA-VA respectively, we observed a similar trend with the strain at break with the diamine having higher elasticity than the triamine. However, in terms of UTS and Young's modulus, J-T-3000-MA-VA showed the lowest values of all the formulations. This is because the J-T-3000 has a high molecular weight, which provides a very soft material when comparing it with lower molecular weight formulations. In the case of J-ED-900-MA-VA, it gives intermediate UTS and Young's modulus values, but the highest strain at break. This can be explained because the structure of the oligomeric J-ED-900 is composed of PEG units that can easily move around each other, being able to relax stress resulting in an elastic material.

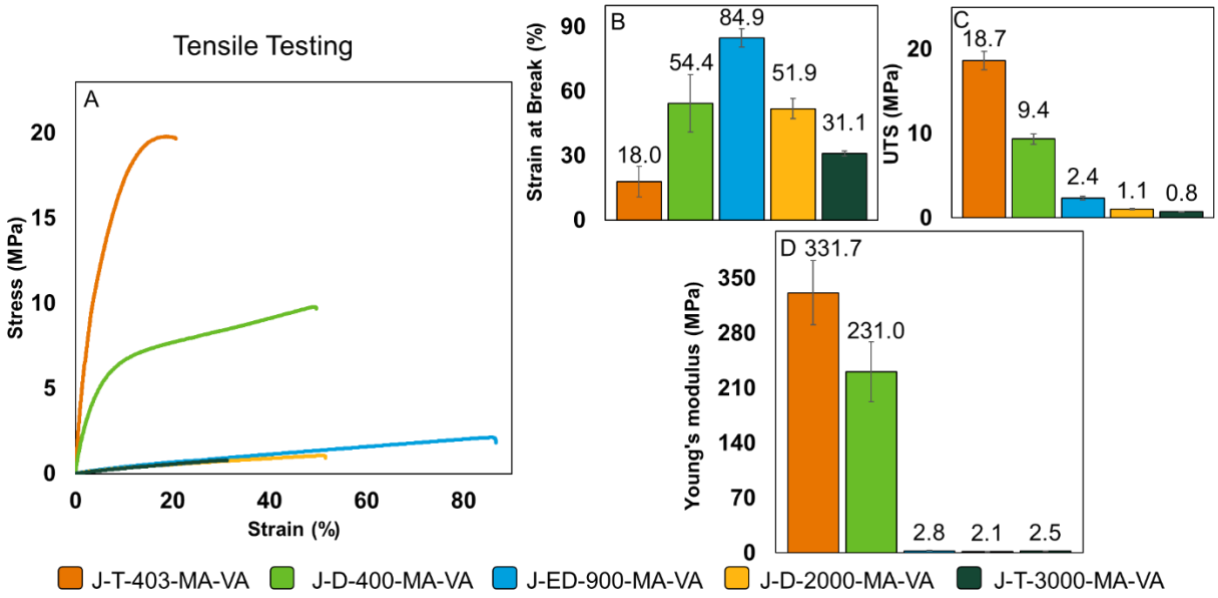

Figure 3. A) Plot of the tensile testing experiments of the five different thermoset formulations. B) Comparison between the strain at break, C) ultimate tensile strength and D) Young's modulus of the five different thermosets.

Additionally, compression testing was conducted to obtain the reprocessing or healing efficiency. Samples were run in triplicate for as printed, annealed and reprocessed samples of the five different formulations. Results of the compressive tests of the as printed samples are shown in Figure S12.

Self-healing and reprocessing

To evaluate the healing behavior, small pieces of each polymer were scratched with a razor blade and then monitored through optical microscopy before and after the thermal treatment at 80°C for 16h. The heat triggered imine exchange reactions, which have been reported to occur readily and without side reactions at temperatures between 50 to 130°C,[51] allow for the rearrangement of the polymer chains to form bonds between the interface of the cut material, and therefore healing the inflicted defects. Two controls without the dynamic crosslinkers were prepared to demonstrate that the healing is caused by the dynamic imine moieties. These controls consisted of VA, cured without crosslinker, and VA cured with 20 mol% of ethylene glycol dimethacrylate as a crosslinker. As seen from the images (Figure 4) the controls showed no healing behavior, however, all five thermoset formulations with the dynamic crosslinkers demonstrated excellent self-healing behaviors with complete disappearance of the inflicted scratches. The only formulation that still showed scarring at the site of the cut was the J-T-403-MA-VA and this can be explained because it has the highest crosslink density. Additional experiments to

evaluate the healing of the crosslinkers cured without any diluent were performed. For this, 2 mL samples of the five methacrylated Jeffamines® were UV-cured and the same procedure for the healing experiments mentioned above were performed. The results showed that the crosslinkers demonstrated efficient healing behaviors after 16h of heating at 80°C, with complete disappearance of the inflicted scratch (Figure S13). However, these crosslinker formulations were too viscous on their own and required curing times that were too long for 3DP.

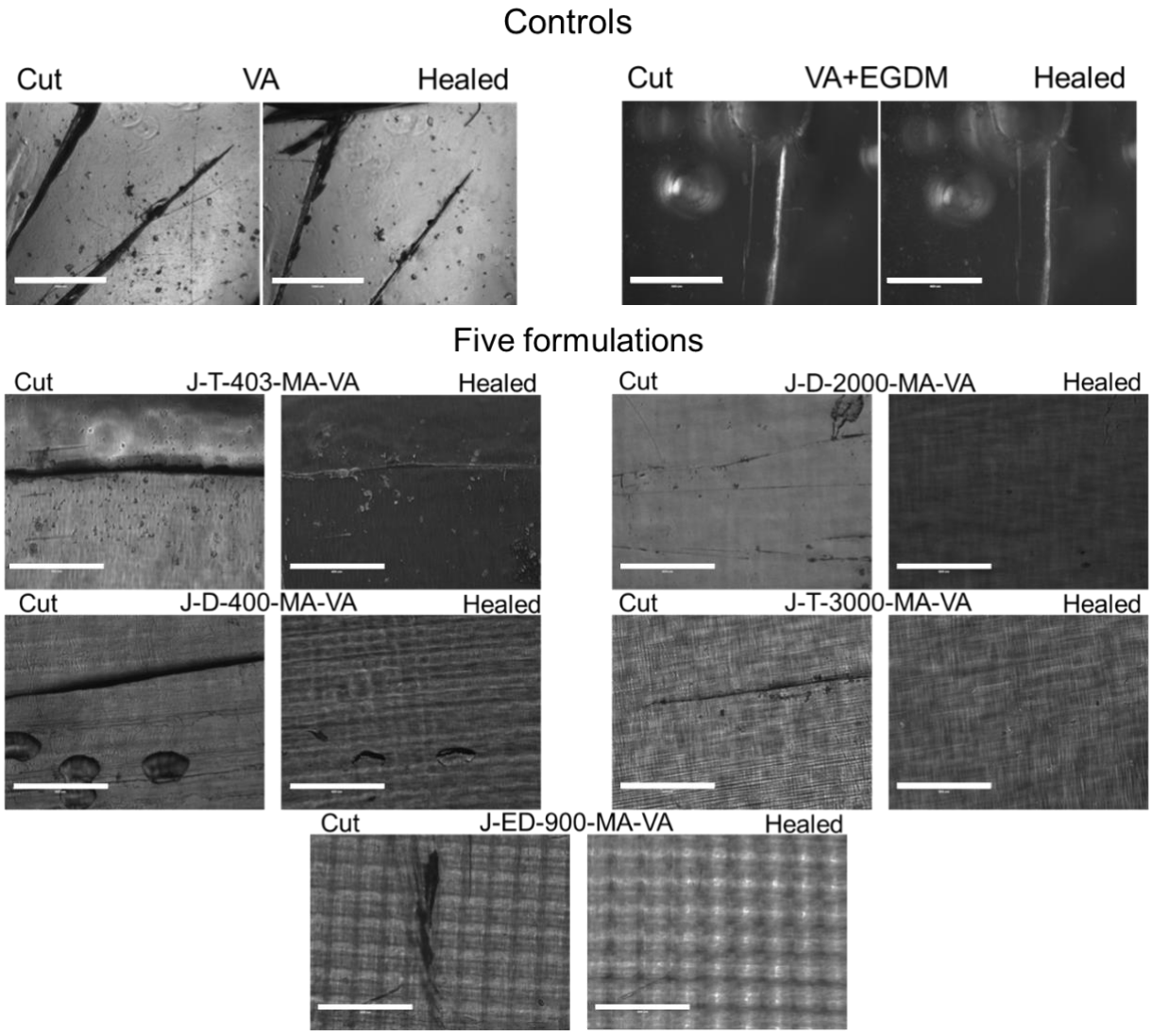

Figure 4. Optical microscopy images of the self-healing experiments for all thermosets (scale bar 400µm).

The presence of the imine moieties also allowed remolding or reprocessing of the materials triggered by heat. All the polymers were readily reprocessed into cylinders with complete incorporation of the material pieces into the new cylinder shape as seen in Figure 5. To qualitatively analyze the incorporation of the fragments into the new shape, microscopy images were obtained of the control and of the five

formulations with the dynamic crosslinkers. As seen in Figure S14, the control still showed the small fragments of the material with an uneven surface, whereas the Jeffamine® formulations showed even incorporation of the pieces, which confirmed their reprocessability.

The healing and reprocessing efficiency was calculated from the comparison between the reprocessed samples and the annealed samples. The results shown in Figure 6 and Figure S15, showed that the property with the highest recovery is the strain at break.

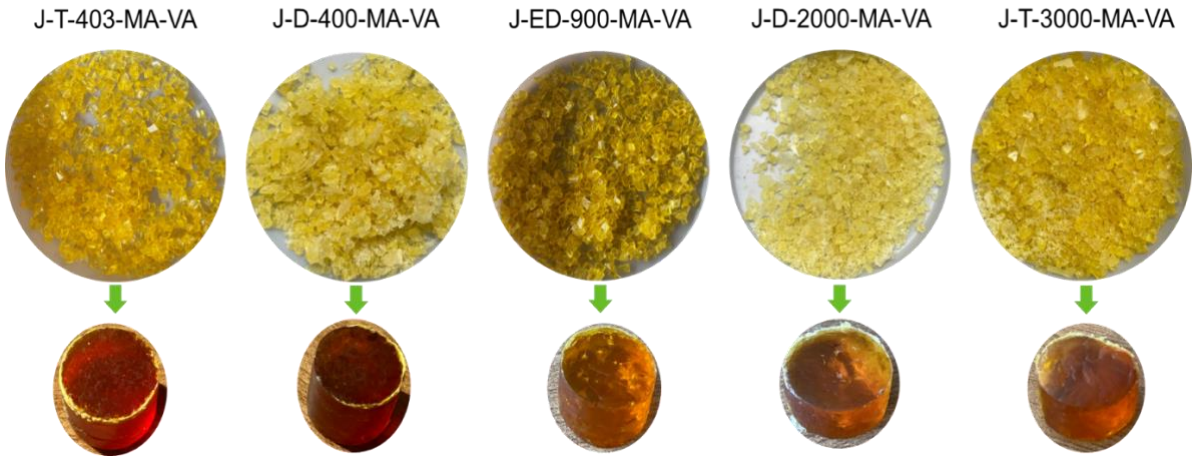

Figure 5. Thermal reprocessing by hot pressing at 140°C and 1500 psi for all five thermoset formulations.

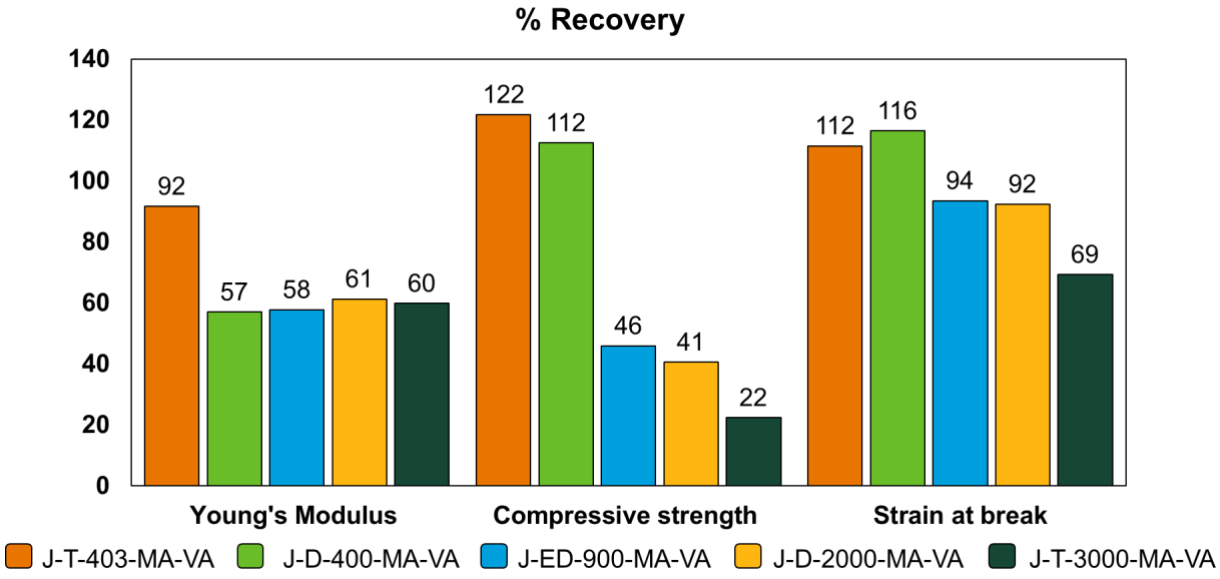

Figure 6. Bar plot comparison of the % recovery of the mechanical properties for all samples after reprocessing.

Chemical degradation experiments

Chemical degradation experiments were performed by placing a small piece (10mg) of each of the five polymers in a 1M solution of hexylamine in THF for three days to break the imine crosslinks and dissolve the polymer. Additionally, a control sample was placed in pure THF which remained practically unchanged (Figure S16). All the polymer samples in hexylamine dissolved and the solution was evaluated through ^{1}H NMR. The spectra showed the characteristic peaks of vanillin, as well as a peak at 8 ppm which corresponded to an imine, likely due to the transimination of hexylamine with the imine crosslinks of the polymer network (Figure S17).

Conclusion

Five 3D printable, self-healable, reprocessable, and chemically degradable thermoset polymers were fabricated by functionalization of different Jeffamines® with VMA and formulated with VA to allow for printability. The addition of VA to the formulations helped reduce the viscosity of the resin, as well as, provided sufficient photopolymerization kinetics to be compatible with DLP 3DP. The five thermosets showed varied mechanical properties (Young's modulus 2.05 – 332 MPa) which indicates a possibility of numerous applications depending on the mechanical requirements. The dynamic imine moieties imparted the polymers with self-healing and reprocessing capabilities through heat-triggered transimination reactions. Microscopy images showed complete disappearance of the inflicted scratches, as well as, complete incorporation of the ground polymer fragments into the new shape after reprocessing. Future work will include more in-depth thermal characterization to quantitatively analyze the vitrimer behavior of these thermoset polymers. Due to the simple synthetic procedures and the commercial availability of Jeffamines®, this series of resins provides a promising alternative to commonly used 3D printable formulations. These advances are necessary in order to shift to materials with predominantly biobased content and to help drift away from polymers made from non-renewable resources.

ASSOCIATED CONTENT

Supporting Information

^{1}H NMR spectra of synthesized monomers and crosslinkers; FTIR spectra of resin formulations; Gel content experiments of formulations in water and ethanol; Strain−stress plot of compression tests of all formulations; Optical microscopy images of self-healing tests of crosslinkers; Optical microscopy images of reprocessed samples and control; Comparison of compression tests of printed, annealed and reprocessed samples; chemical degradation tests of the five formulations, ^{1}H NMR spectra of the chemical degradation experiments.

AUTHOR INFORMATION

Corresponding Author

Ronald A. Smaldone − Department of Chemistry and Biochemistry, Department of Materials Science and Engineering, University of Texas at Dallas, Richardson, Texas 75080, United States; orcid.org/0000-0003-4560-7079
Email: ronald.smaldone@utdallas.edu

Authors

Karen P. Cortés-Guzmán−Department of Chemistry and Biochemistry, University of Texas at Dallas, Richardson, Texas 75080, United States;orcid.org/0000-0002-8793-4687

Ankit R. Parikh − Department of Mechanical Engineering, University of Texas at Dallas, Richardson, Texas 75080, United States; orcid.org/0000-0003-0107-5533

Marissa L. Sparacin − Department of Chemistry and Biochemistry, University of Texas at Dallas, Richardson, Texas 75080, United States; orcid.org/ 0000-0003-2500-8239

Ashele K. Remy − Department of Chemistry and Biochemistry, University of Texas at Dallas, Richardson, Texas 75080, United States; orcid.org/ 0000-0001-9221-0862

Walter E. Voit − Department of Biological Sciences and Department of Materials Science and Engineering, The University of Texas at Dallas, 800 W Campbell Road, Richardson, Texas 75080, United States; orcid.org/0000-0003-0135-0531

Lauren Adegoke − Department of Biomedical Engineering, University of North Texas, Denton, Texas 75203, United States; orcid.org/0000-0001-8513-4160

Melanie Ecker − Department of Biomedical Engineering, University of North Texas, Denton, Texas 75203, United States; orcid.org/0000-0002-0603-6683

Chandani Chitrakar − Department of Biomedical Engineering, University of North Texas, Denton, Texas 75203, United States; orcid.org/0000-0003-2956-9527

Notes

The authors declare no competing financial interest.

Author Contributions

The manuscript was written through contributions of all authors. All authors have given approval to the final version of the manuscript.

ACKNOWLEDGMENTS

Funding Sources

K.C.G. acknowledges the Consejo Nacional de Ciencia y Tecnología (CONACYT, Mexican Council of Science and Technology) for doctoral fellowship. We also acknowledge the Advanced Polymer Research Lab (APRL) at UT Dallas for access to facilities for the thermal characterization of polymers. UT Dallas. A.K.P. acknowledges scientific and internship support from the U.S. Food and Drug Administration. R.A.S. acknowledges support from UT Dallas, and the Army Research Laboratory (W911NF-18-2-0035) and the American Chemical Society Petroleum Research Fund (PRF#61360- ND10).

References

(1) Stuchtey, M.; MacArthur, D.; Dominic, W. *The New Plastics Economy Rethinking the Future of Plastics*; 2016.

(2) Nielsen, T. D.; Hasselbalch, J.; Holmberg, K.; Stripple, J. Politics and the Plastic Crisis: A Review throughout the Plastic Life Cycle. *WIREs Energy Environ.* **2019**, *9*, 1–18. https://doi.org/10.1002/wene.360.

(3) Mülhaupt, R. Green Polymer Chemistry and Bio-Based Plastics: Dreams and Reality. *Macromol. Chem. Phys.* **2013**, *214*, 159–174. https://doi.org/10.1002/macp.201200439.

(4) Fache, M.; Auvergne, R.; Boutevin, B.; Caillol, S. New Vanillin-Derived Diepoxy Monomers for the Synthesis of Biobased Thermosets. *Eur. Polym. J.* **2015**, *67*, 527–538. https://doi.org/10.1016/j.eurpolymj.2014.10.011.

(5) Stanzione, J. F.; Sadler, J. M.; La Scala, J. J.; Reno, K. H.; Wool, R. P. Vanillin-Based Resin for Use in Composite Applications. *Green Chem.* **2012**, *14*, 2346–2352. https://doi.org/10.1039/c2gc35672d.

(6) Fache, M.; Boutevin, B.; Caillol, S. Vanillin Production from Lignin and Its Use as a Renewable Chemical. *ACS Sustain. Chem. Eng.* **2016**, *4*, 35–46. https://doi.org/10.1021/acssuschemeng.5b01344.

(7) Fagnani, D. E.; Tami, J. L.; Copley, G.; Clemons, M. N.; Getzler, Y. D. Y. L.; McNeil, A. J. 100th Anniversary of Macromolecular Science Viewpoint: Redefining Sustainable Polymers. *ACS Macro Lett.* **2021**, *10,* 41–53. https://doi.org/10.1021/acsmacrolett.0c00789.

(8) White, S. R.; Sottos, N. R.; Geubelle, P. H.; Moore, J. S.; Kessler, M. R.; Sriram, S. R.; Brown, E. N.; Viswanathan, S. "Autonomic Healing of Polymer Composites," *Nature* **2001**, *409*, 794-797. https://doi.org/10.1038/35057232

(9) Wang, S.; Urban, M. W. Self-Healing Polymers. *Nat. Rev. Mater.* **2020**, *5*, 562–583. https://doi.org/10.1038/s41578-020-0202-4.

(10) Chen, X.; Dam, M. A.; Ono, K.; Mal, A.; Shen, H.; Nutt, S. R.; Sheran, K.; Wudl,

F. A Thermally Re-Mendable Cross-Linked Polymeric Material. *Science* **2002**, *295*, 1698–1702. https://doi.org/10.1126/science.1065879.

(11) Dahlke, J.; Zechel, S.; Hager, M. D.; Schubert, U. S. How to Design a Self-Healing Polymer: General Concepts of Dynamic Covalent Bonds and Their Application for Intrinsic Healable Materials. *Adv. Mater. Interfaces* **2018**, *5*. https://doi.org/10.1002/admi.201800051.

(12) Herbst, F.; Döhler, D.; Michael, P.; Binder, W. H. Self-Healing Polymers *via* Supramolecular Forces. *Macromol. Rapid Commun.* **2013**, *34*, 203–220. https://doi.org/10.1002/marc.201200675.

(13) Jiménez, M.; Romero, L.; Domínguez, I. A.; Espinosa, M. D. M.; Domínguez, M. Additive Manufacturing Technologies: An Overview about 3D Printing Methods and Future Prospects. *Complexity* **2019**, *2019*, 1–30. https://doi.org/10.1155/2019/9656938.

(14) Sanchez-Rexach, E.; Johnston, T. G.; Jehanno, C.; Sardon, H.; Nelson, A. Sustainable Materials and Chemical Processes for Additive Manufacturing. *Chem. Mater.* **2020**, *32*, 7105–7119. https://doi.org/10.1021/acs.chemmater.0c02008.

(15) Berry, D. R.; Cortés-Guzmán, K. P.; Durand-Silva, A.; Perera, S. D.; Remy, A. K.; Yan, Q.; Smaldone, R. A. Supramolecular Tools for Polymer Additive Manufacturing. *MRS Commun.* **2021**, *11*, 146–156. https://doi.org/10.1557/s43579-021-00037-9.

(16) Stansbury, J. W.; Idacavage, M. J. 3D Printing with Polymers: Challenges among Expanding Options and Opportunities. *Dent. Mater.* **2016**, *32*, 54–64. https://doi.org/10.1016/j.dental.2015.09.018.

(17) Berman, B. 3-D Printing: The New Industrial Revolution. *Bus. Horiz.* **2012**, *55*, 155–162. https://doi.org/10.1016/j.bushor.2011.11.003.

(18) Kloxin, C. J.; Bowman, C. N. Covalent Adaptable Networks: Smart, Reconfigurable and Responsive Network Systems. *Chem. Soc. Rev.* **2013**, *42*, 7161–7173. https://doi.org/10.1039/c3cs60046g.

(19) Lyon, G. B.; Baranek, A.; Bowman, C. N. Scaffolded Thermally Remendable Hybrid Polymer Networks. *Adv. Funct. Mater.* **2016**, *26*, 1477–1485. https://doi.org/10.1002/adfm.201505368.

(20) Sheppard, D. T.; Jin, K.; Hamachi, L. S.; Dean, W.; Fortman, D. J.; Ellison, C. J.; Dichtel, W. R. Reprocessing Postconsumer Polyurethane Foam Using Carbamate Exchange Catalysis and Twin-Screw Extrusion. *ACS Cent. Sci.* **2020**, *6*, 921–927. https://doi.org/10.1021/acscentsci.0c00083.

(21) Kloxin, C. J.; Scott, T. F.; Adzima, B. J.; Bowman, C. N. Covalent Adaptable Networks (CANs): A Unique Paradigm in Cross-Linked Polymers. *Macromolecules* **2010**, *43*, 2643–2653. https://doi.org/10.1021/ma902596s.

(22) Scheutz, G. M.; Lessard, J. J.; Sims, M. B.; Sumerlin, B. S. Adaptable

Crosslinks in Polymeric Materials: Resolving the Intersection of Thermoplastics and Thermosets. *J. Am. Chem. Soc.* **2019**, *141*, 16181–16196. https://doi.org/10.1021/jacs.9b07922.

(23) Krishnakumar, B.; Sanka, R. V. S. P.; Binder, W. H.; Parthasarthy, V.; Rana, S.; Karak, N. Vitrimers: Associative Dynamic Covalent Adaptive Networks in Thermoset Polymers. *Chem. Eng. J.* **2019**, *385*, 123820. https://doi.org/10.1016/j.cej.2019.123820.

(24) Tao, Y.; Fang, L.; Zhou, J.; Wang, C.; Sun, J.; Fang, Q. Gel–Sol Transition of Vanillin-Based Polyimine Vitrimers: Imparting Vitrimers with Extra Welding and Self-Healing Abilities. *ACS Appl. Polym. Mater.* **2020**, *2*, 295–303. https://doi.org/10.1021/acsapm.9b00809.

(25) Ma, Z.; Wang, Y.; Zhu, J.; Yu, J.; Hu, Z. Bio-Based Epoxy Vitrimers: Reprocessibility, Controllable Shape Memory, and Degradability. *J. Polym. Sci. Part A Polym. Chem.* **2017**, *55*, 1790–1799. https://doi.org/10.1002/pola.28544.

(26) Wu, J.; Yu, X.; Zhang, H.; Guo, J.; Hu, J.; Li, M.-H. Fully Biobased Vitrimers from Glycyrrhizic Acid and Soybean Oil for Self-Healing, Shape Memory, Weldable, and Recyclable Materials. *ACS Sustain. Chem. Eng.* **2020**, *8*, 6479–6487. https://doi.org/10.1021/acssuschemeng.0c01047.

(27) Shi, Q.; Yu, K.; Kuang, X.; Mu, X.; Dunn, C. K.; Dunn, M. L.; Wang, T.; Jerry Qi, H. Recyclable 3D Printing of Vitrimer Epoxy. *Mater. Horiz.* **2017**, *4*, 598–607. https://doi.org/10.1039/C7MH00043J.

(28) He, X.; Lei, Z.; Zhang, W.; Yu, K. Recyclable 3D Printing of Polyimine-Based Covalent Adaptable Network Polymers. *3D Print. Addit. Manuf.* **2019**, *6*, 31–39. https://doi.org/10.1089/3dp.2018.0115.

(29) Maines, E. M.; Porwal, M. K.; Ellison, C. J.; Reineke, T. M. Sustainable Advances in SLA DLP 3D Printing Materials and Processes. *Green Chem.* **2021**, *23*, 6863–6897. https://doi.org/10.1039/d1gc01489g.

(30) Yuan, T.; Zhang, L.; Li, T.; Tu, R.; Sodano, H. A. 3D Printing of a Self-Healing, High Strength, and Reprocessable Thermoset. *Polym. Chem.* **2020**, *11*, 6441–6452.

(31) Davidson, J. R.; Appuhamillage, G. A.; Thompson, C. M.; Voit, W.; Smaldone, R. A. Design Paradigm Utilizing Reversible Diels-Alder Reactions to Enhance the Mechanical Properties of 3D Printed Materials. *ACS Appl. Mater. Interfaces* **2016**, *8*, 16961–16966. https://doi.org/10.1021/acsami.6b05118.

(32) Appuhamillage, G. A.; Reagan, J. C.; Khorsandi, S.; Davidson, J. R.; Voit, W.; Smaldone, R. A. 3D Printed Remendable Polylactic Acid Blends with Uniform Mechanical Strength Enabled by a Dynamic Diels-Alder Reaction. *Polym. Chem.* **2017**, *8*, 2087–2092. https://doi.org/10.1039/c7py00310b.

(33) Yang, K.; Grant, J. C.; Lamey, P.; Joshi-Imre, A.; Lund, B. R.; Smaldone, R.

A.; Voit, W. Diels–Alder Reversible Thermoset 3D Printing: Isotropic Thermoset Polymers via Fused Filament Fabrication. *Adv. Funct. Mater.* **2017**, *27*, 1700318. https://doi.org/10.1002/adfm.201700318.

(34) Li, X.; Yu, R.; He, Y.; Zhang, Y.; Yang, X.; Zhao, X.; Huang, W. Self-Healing Polyurethane Elastomers Based on a Disulfide Bond by Digital Light Processing 3D Printing. *ACS Macro Lett.* **2019**, *8,* 1511–1516. https://doi.org/10.1021/acsmacrolett.9b00766.

(35) Li, X.; Yu, R.; He, Y.; Zhang, Y.; Yang, X.; Zhao, X. Four-Dimensional Printing of Shape Memory Polyurethanes with High Strength and Recyclability Based on Diels-Alder Chemistry. *Polymer* **2020**, *200*, 122532. https://doi.org/10.1016/j.polymer.2020.122532.

(36) Durand-Silva, A.; Cortés-Guzmán, K. P.; Johnson, R. M.; Perera, S. D.; Diwakara, S. D.; Smaldone, R. A. Balancing Self-Healing and Shape Stability in Dynamic Covalent Photoresins for Stereolithography 3D Printing. *ACS Macro Lett.* **2021**, *10*, 486–491. https://doi.org/10.1021/acsmacrolett.1c00121.

(37) Zhang, B.; Kowsari, K.; Serjouei, A.; Dunn, M. L.; Ge, Q. Reprocessable Thermosets for Sustainable Three-Dimensional Printing. *Nat. Commun.* **2018**, *9*, 1831. https://doi.org/10.1038/s41467-018-04292-8.

(38) Liu, T.; Zhao, B.; Zhang, J. Recent Development of Repairable, Malleable and Recyclable Thermosetting Polymers through Dynamic Transesterification. *Polymer* **2020**, *194*, 122392. https://doi.org/10.1016/j.polymer.2020.122392.

(39) García, F.; Smulders, M. M. J. Dynamic Covalent Polymers. *J. Polym. Sci. Part A Polym. Chem.* **2016**, *54*, 3551–3577. https://doi.org/10.1002/pola.28260.

(40) Chao, A.; Negulescu, I.; Zhang, D. Dynamic Covalent Polymer Networks Based on Degenerative Imine Bond Exchange: Tuning the Malleability and Self-Healing Properties by Solvent. *Macromolecules* **2016**, *49*, 6277–6284. https://doi.org/10.1021/acs.macromol.6b01443.

(41) Skene, W. G.; Lehn, J. M. P. Dynamers: Polyacylhydrazone Reversible Covalent Polymers, Component Exchange, and Constitutional Diversity. *Proc. Natl. Acad. Sci. U. S. A.* **2004**, *101*, 8270–8275. https://doi.org/10.1073/pnas.0401885101.

(42) Miao, J. T.; Ge, M.; Peng, S.; Zhong, J.; Li, Y.; Weng, Z.; Wu, L.; Zheng, L. Dynamic Imine Bond-Based Shape Memory Polymers with Permanent Shape Reconfigurability for 4D Printing. *ACS Appl. Mater. Interfaces* **2019**, *11*, 40642–40651. https://doi.org/10.1021/acsami.9b14145.

(43) Wang, L. L.; Highley, C. B.; Yeh, Y. C.; Galarraga, J. H.; Uman, S.; Burdick, J. A. Three-Dimensional Extrusion Bioprinting of Single- and Double-Network Hydrogels Containing Dynamic Covalent Crosslinks. *J. Biomed. Mater. Res., Part A* **2018**, *106*, 865–875. https://doi.org/10.1002/jbm.a.36323.

(44) Mo, R.; Song, L.; Hu, J.; Sheng, X.; Zhang, X. An Acid-Degradable Biobased

Epoxy-Imine Adaptable Network Polymer for the Fabrication of Responsive Structural Color Film. *Polym. Chem.* **2020**, *11*, 974–981. https://doi.org/10.1039/c9py01821b.

(45) Geng, H.; Wang, Y.; Yu, Q.; Gu, S.; Zhou, Y.; Xu, W.; Zhang, X.; Ye, D. Vanillin-Based Polyschiff Vitrimers: Reprocessability and Chemical Recyclability. *ACS Sustain. Chem. Eng.* **2018**, *6*, 15463–15470. https://doi.org/10.1021/acssuschemeng.8b03925.

(46) Zhang, D. D.; Ruan, Y. B.; Zhang, B. Q.; Qiao, X.; Deng, G.; Chen, Y.; Liu, C. Y. A Self-Healing PDMS Elastomer Based on Acylhydrazone Groups and the Role of Hydrogen Bonds. *Polymer* **2017**, *120*, 189–196. https://doi.org/10.1016/j.polymer.2017.05.060.

(47) Xu, Y.; Odelius, K.; Hakkarainen, M. Photocurable, Thermally Reprocessable, and Chemically Recyclable Vanillin-Based Imine Thermosets. *ACS Sustain. Chem. Eng.* **2020**, *8*, 17272–17279. https://doi.org/10.1021/acssuschemeng.0c06248.

(48) Genest, A.; Portinha, D.; Fleury, E.; Ganachaud, F. The Aza-Michael Reaction as an Alternative Strategy to Generate Advanced Silicon-Based (Macro)Molecules and Materials. *Prog. Polym. Sci.* **2017**, *72*, 61–110. https://doi.org/10.1016/j.progpolymsci.2017.02.002.

(49) Zhou, J.; Zhang, H.; Deng, J.; Wu, Y. High Glass-Transition Temperature Acrylate Polymers Derived from Biomasses, Syringaldehyde, and Vanillin. *Macromol. Chem. Phys.* **2016**, *217*, 2402–2408. https://doi.org/10.1002/macp.201600305.

(50) Abdelaty, M. S. A. Influence of Vanillin Acrylate and 4-Acetylphenyl Acrylate Hydrophobic Functional Monomers on Phase Separation of N-Isopropylacrylamide Environmental Terpolymer: Fabrication and Characterization. *Polym. Bull.* **2020**, *77*, 2905–2922. https://doi.org/10.1007/s00289-019-02890-0.

(51) Elling, B. R.; Dichtel, W. R. Reprocessable Cross-Linked Polymer Networks: Are Associative Exchange Mechanisms Desirable? *ACS Cent. Sci.* **2020**, *6,* 1488–1496. https://doi.org/10.1021/acscentsci.0c00567.

Recyclable, Biobased Photoresins for 3D Printing through Dynamic Imine Exchange

Karen P. Cortés-Guzmán,[1] Ankit R. Parikh,[2] Marissa L. Sparacin,[1] Ashele K. Remy,[1] Lauren Adegoke,[4] Chandani Chitrakar,[4] Melanie Ecker,[4] Walter E. Voit,[2,3] Ronald A. Smaldone*[1,3]

[1]Department of Chemistry and Biochemistry, University of Texas at Dallas, 800 West Campbell Road, Richardson, Texas 75080, United States

[2]Department of Mechanical Engineering UT Dallas University of Texas at Dallas, 800 West Campbell Road, Richardson, Texas 75080, United States

[3]Department of Materials Science and Engineering UT Dallas University of Texas at Dallas, 800 West Campbell Road, Richardson, Texas 75080, United States

[4]Department of Biomedical Engineering, University of North Texas, 1155 Union Circle #310440, Denton, Texas 75203, United States

Table of contents

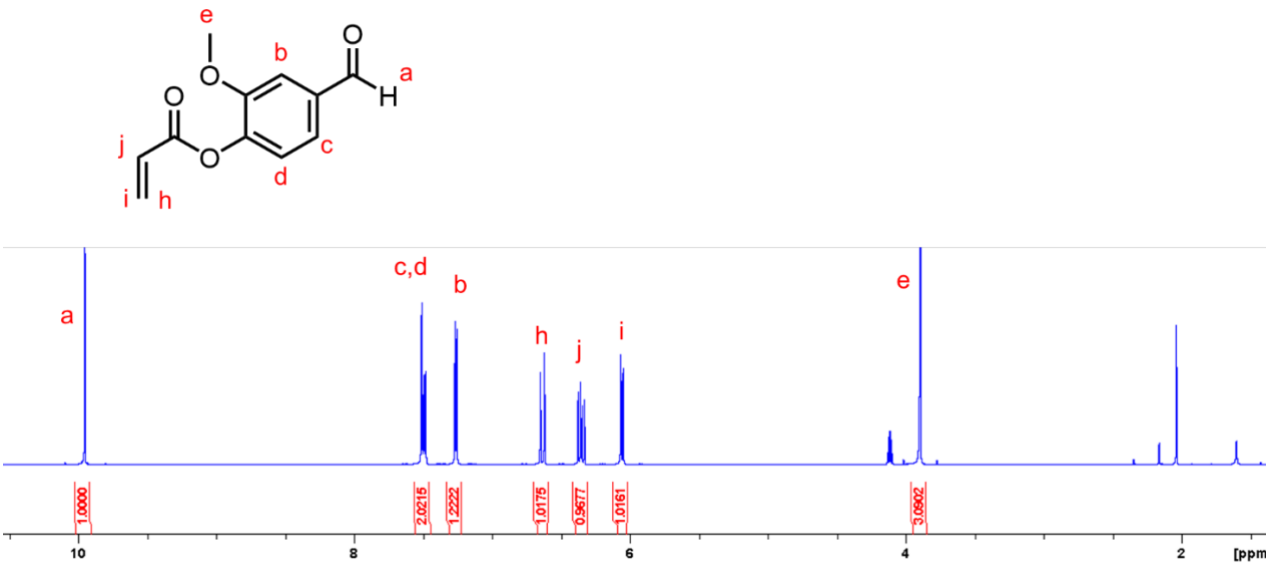

Figure S1. ^{1}H NMR Vanillin Acrylate in $CDCl_3$.

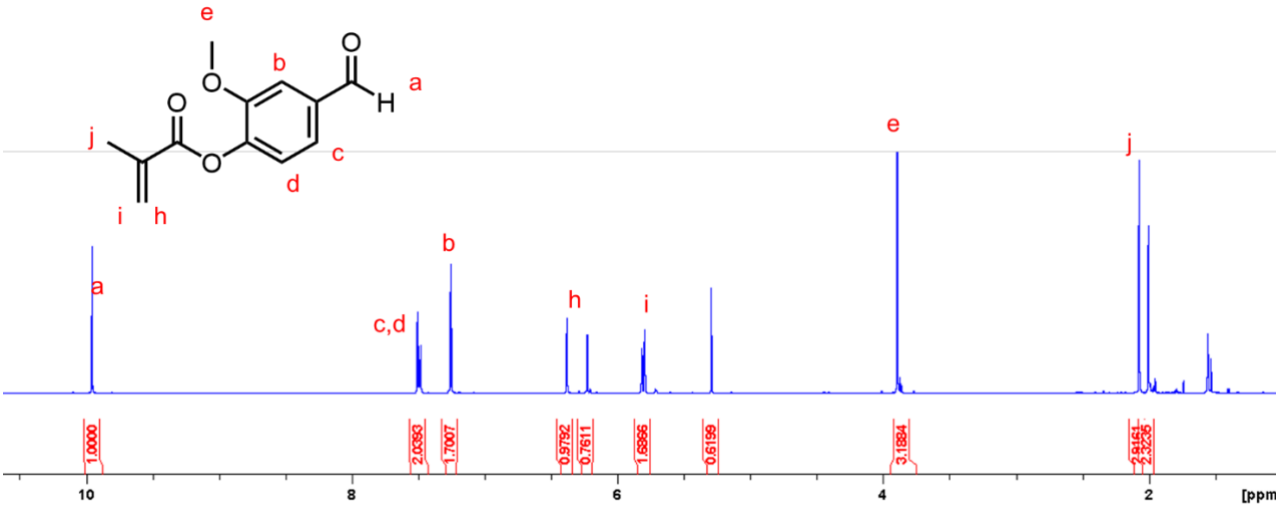

Figure S2. ^{1}H NMR Vanillin Methacrylate in $CDCl_3$.

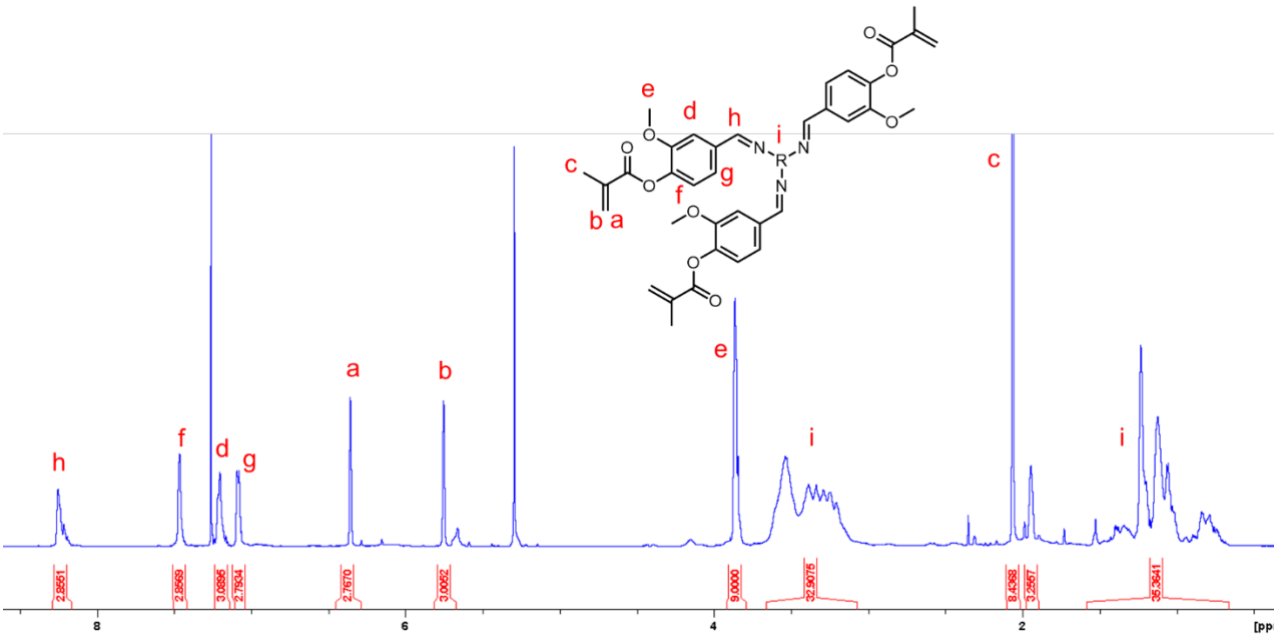

Figure S3. ^{1}H NMR Jeffamine® T-403 methacrylate (J-T-403-MA) in $CDCl_3$.

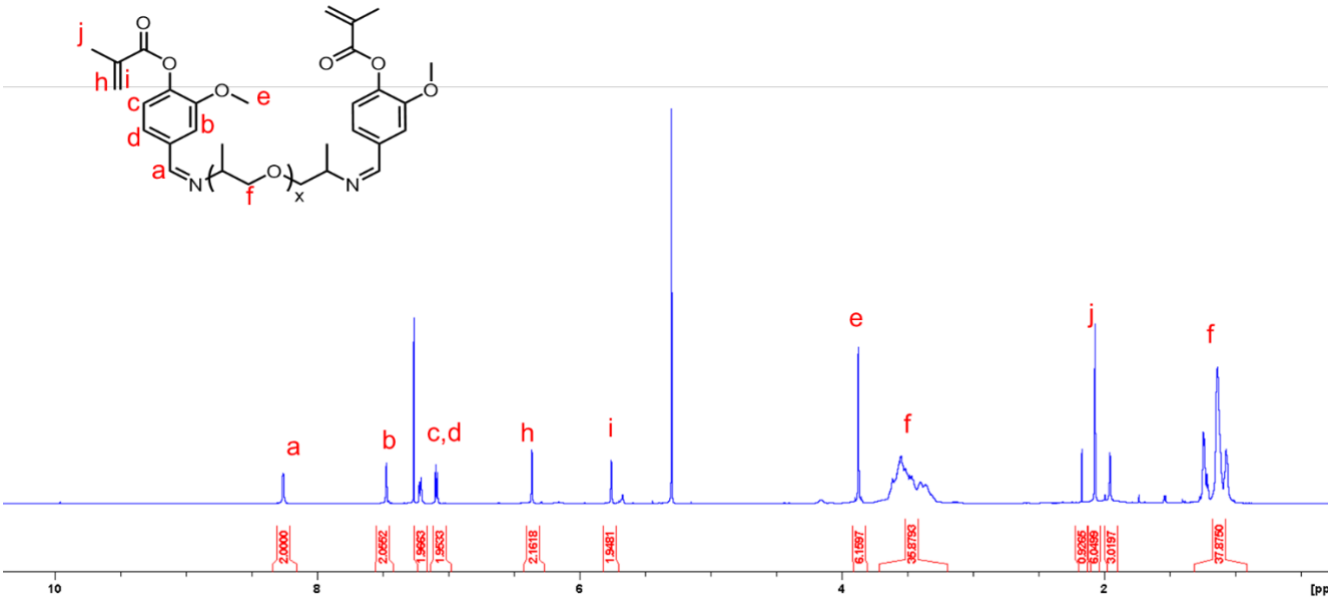

Figure S4. ^{1}H NMR Jeffamine® D-400 methacrylate (J-D-400-MA) in $CDCl_3$.

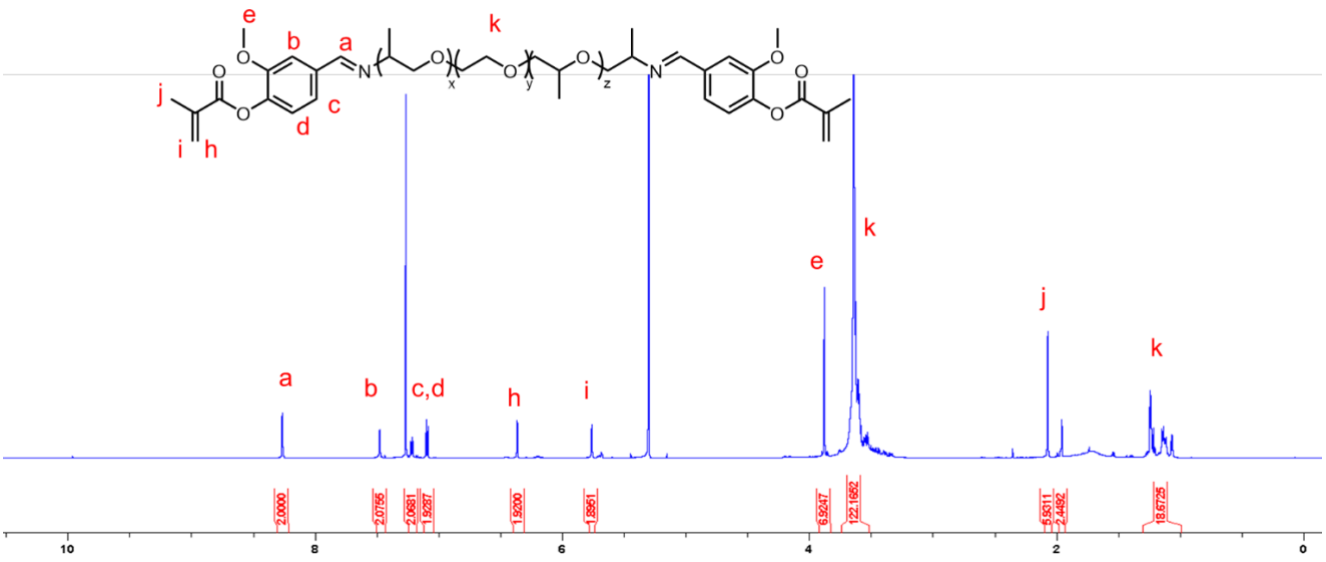

Figure S5. ^{1}H NMR Jeffamine® ED-900 methacrylate (J-ED-900-MA) in $CDCl_3$.

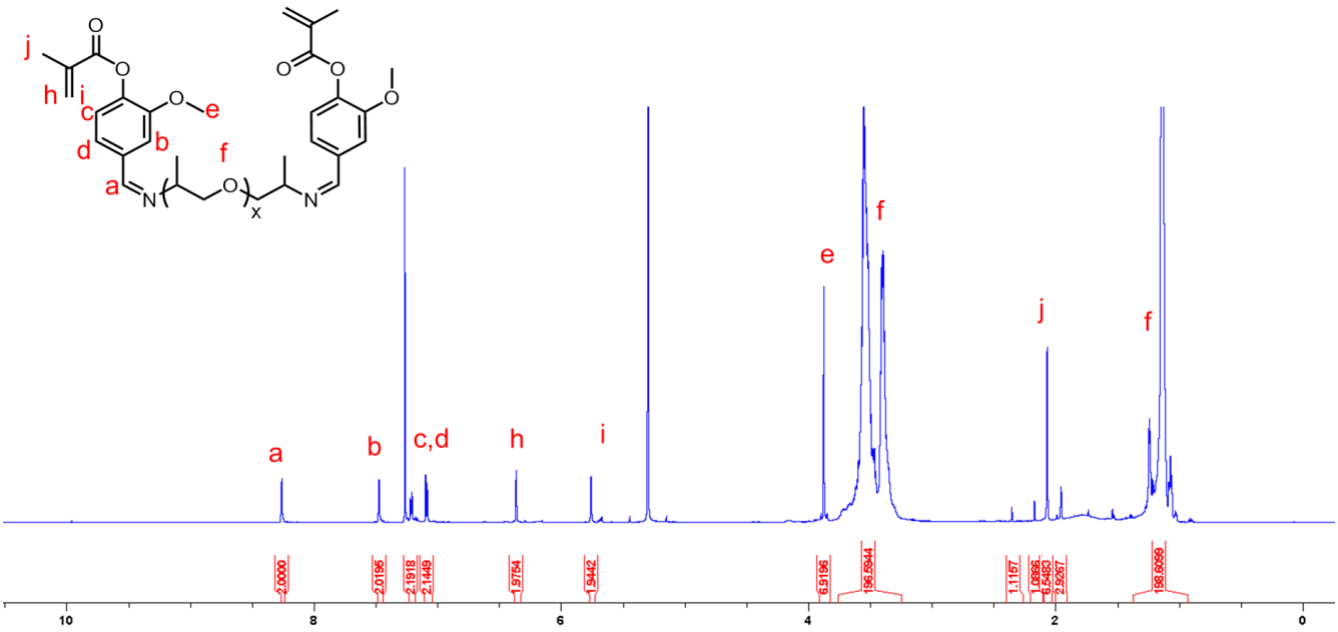

Figure S6. ^{1}H NMR Jeffamine® D-2000 methacrylate (J-D-2000-MA) in $CDCl_3$.

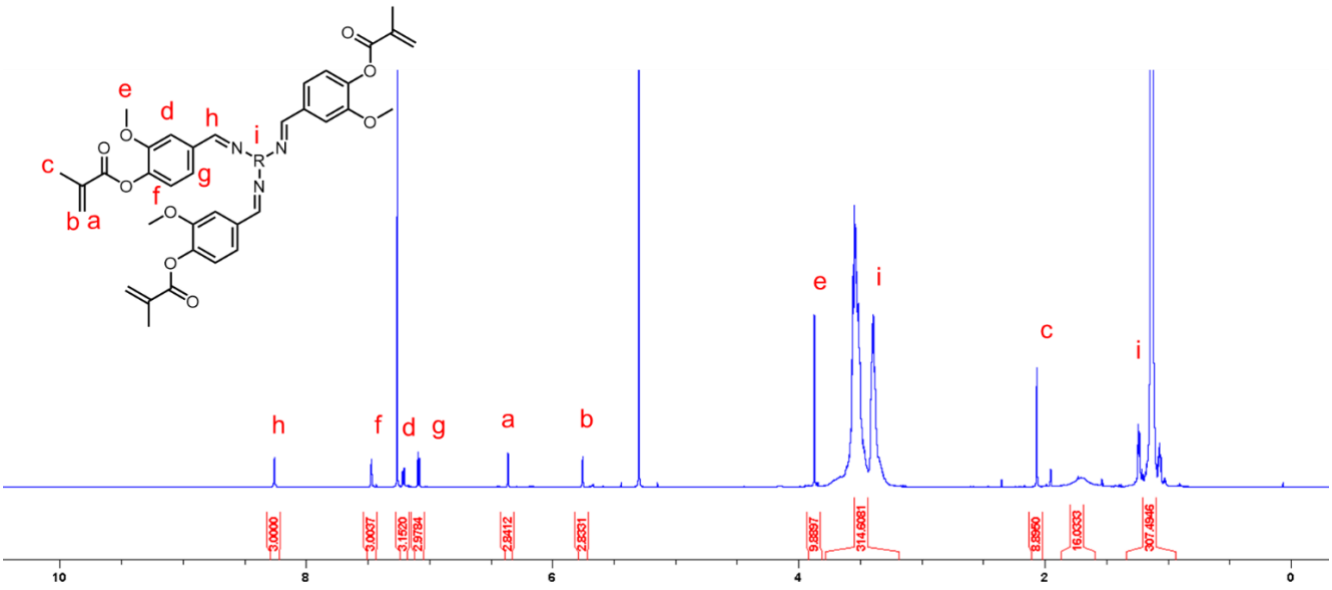

Figure S7. ^{1}H NMR Jeffamine® T-3000 methacrylate (J-T-3000-MA) in $CDCl_3$.

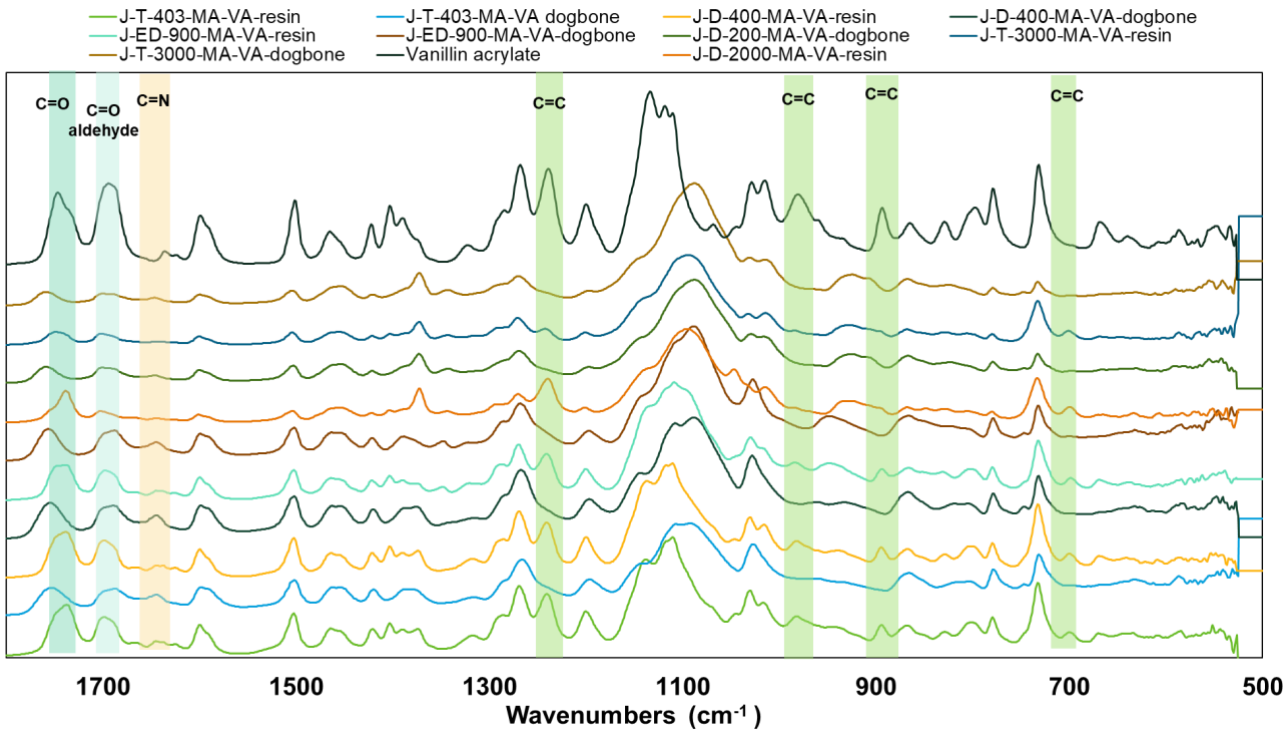

Figure S8. FTIR spectra of resins and cured polymer formulations.

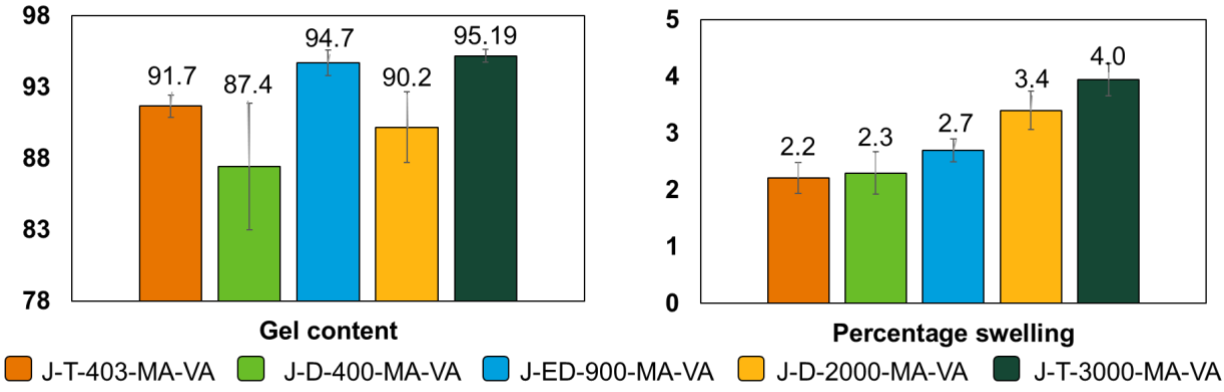

Figure S9. Gel content and swelling experiments in ethanol for 3 days.

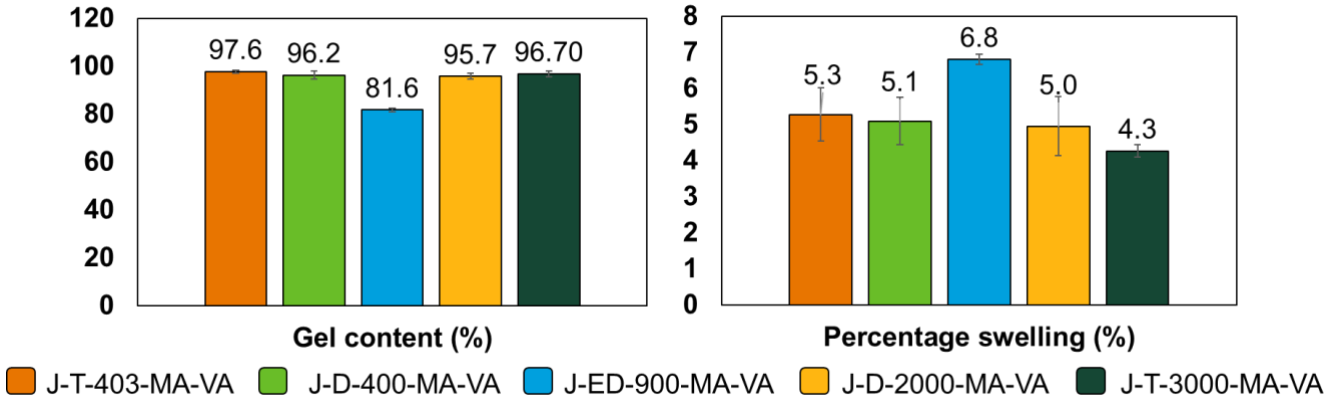

Figure S10. Gel content and swelling experiments in water for 3 days.

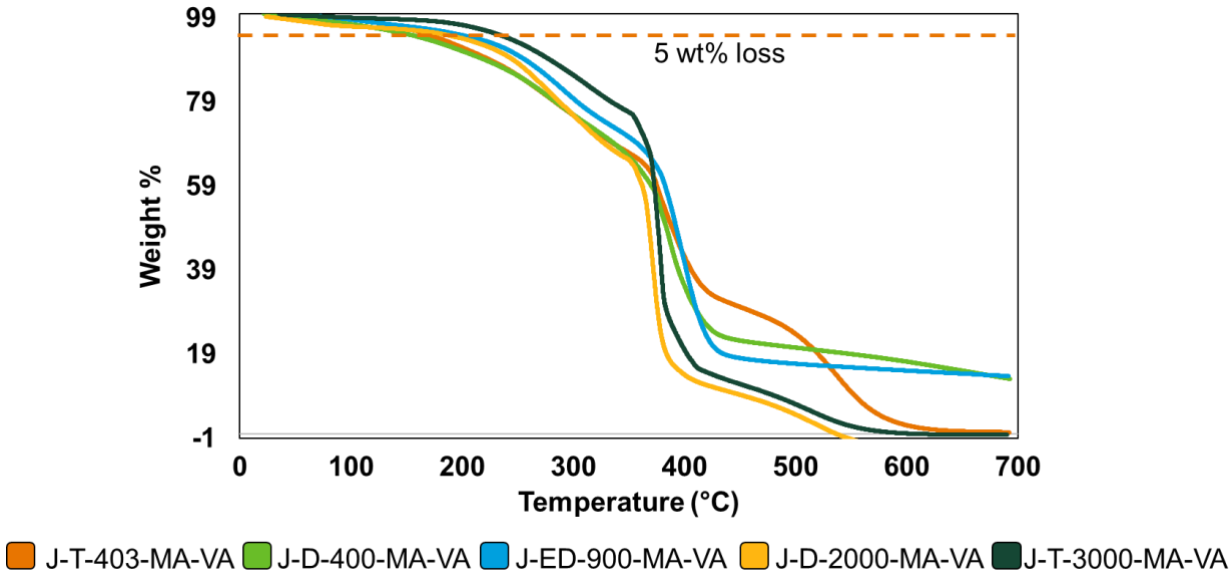

Figure S11. Thermogravimetric analysis of the five thermosets.

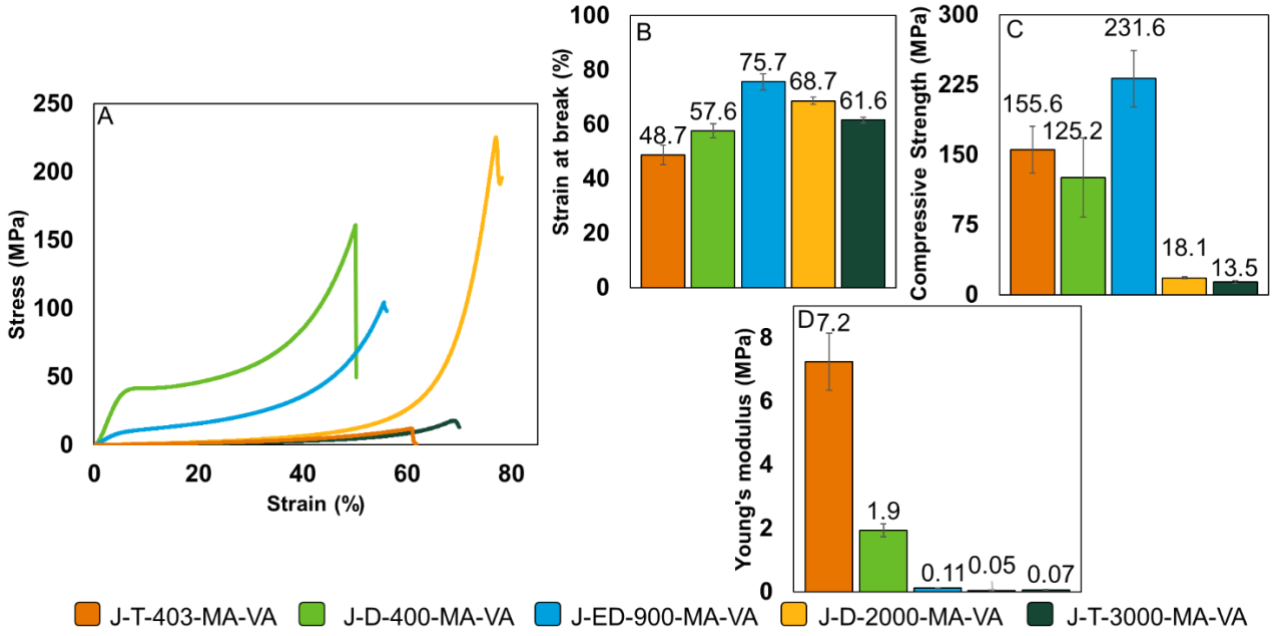

Figure S12. A) Plot of the compressive testing experiments of the five different thermoset formulations. B) Comparison between the strain at break, C) Compressive strength and D) Young's modulus of the five different thermosets.

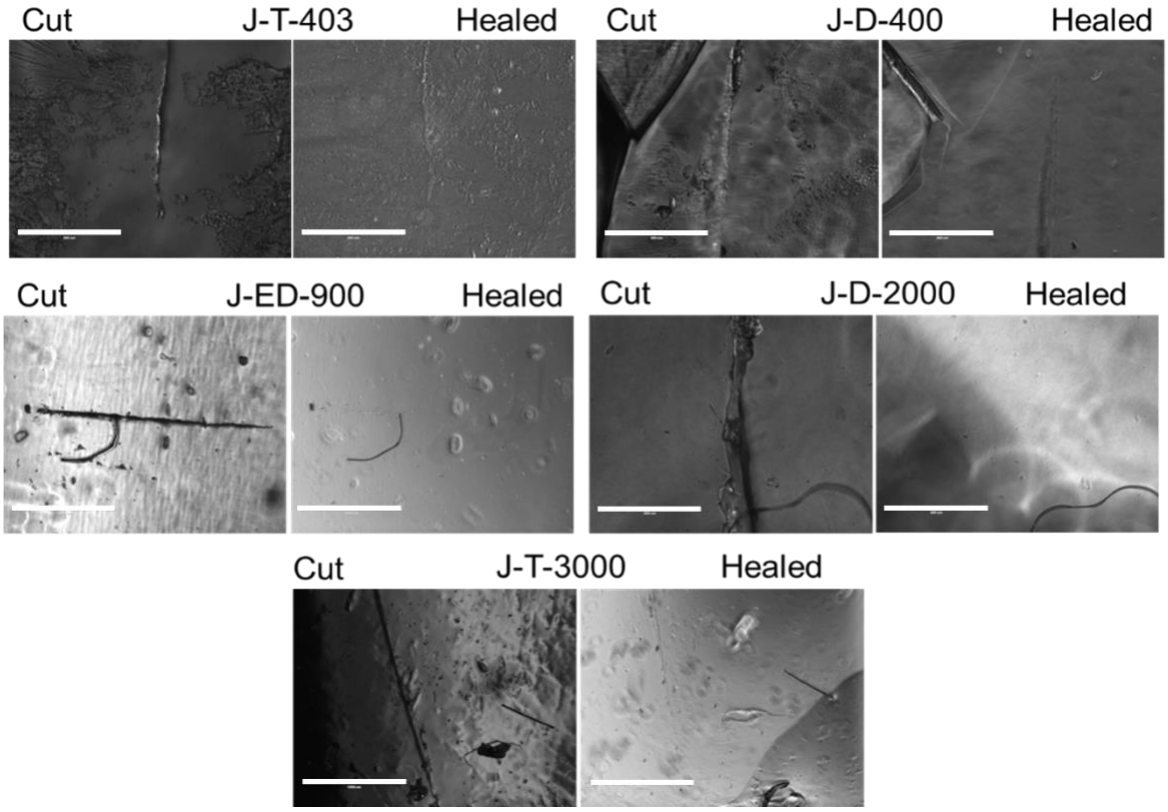

Figure S13. Optical microscopy images of the self-healing of the five thermosets without any reactive diluent (scale bar 400μm).

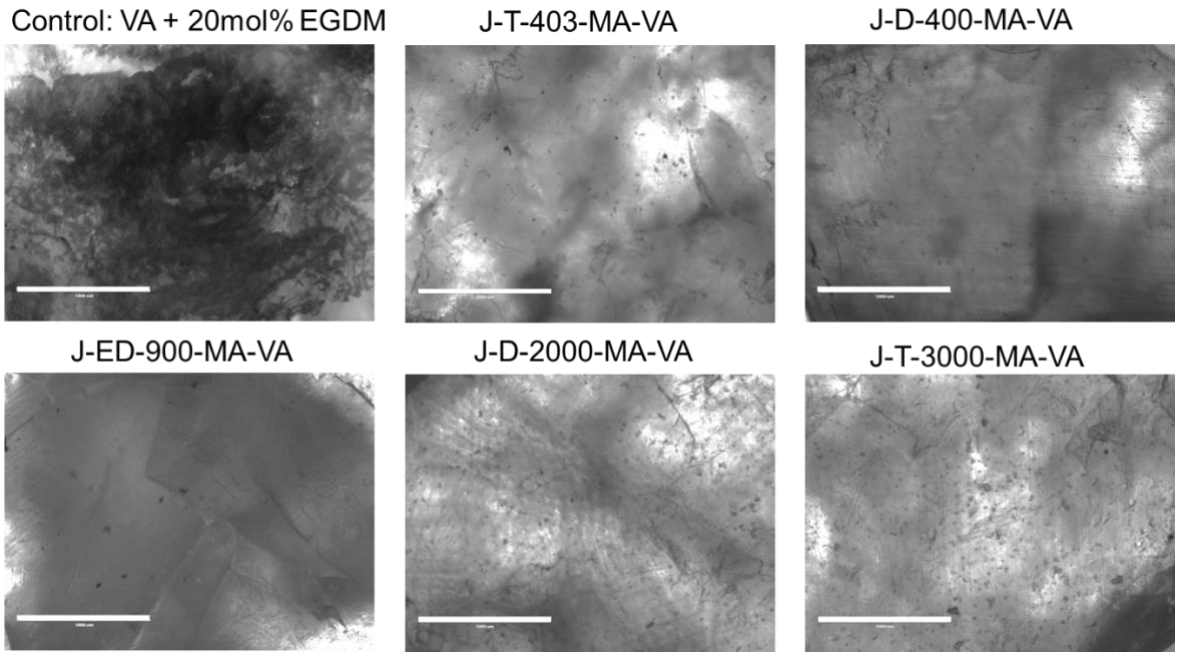

Figure S14. Optical microscopy images of the reprocessing of the five thermoset formulations (scale bar 1000μm).

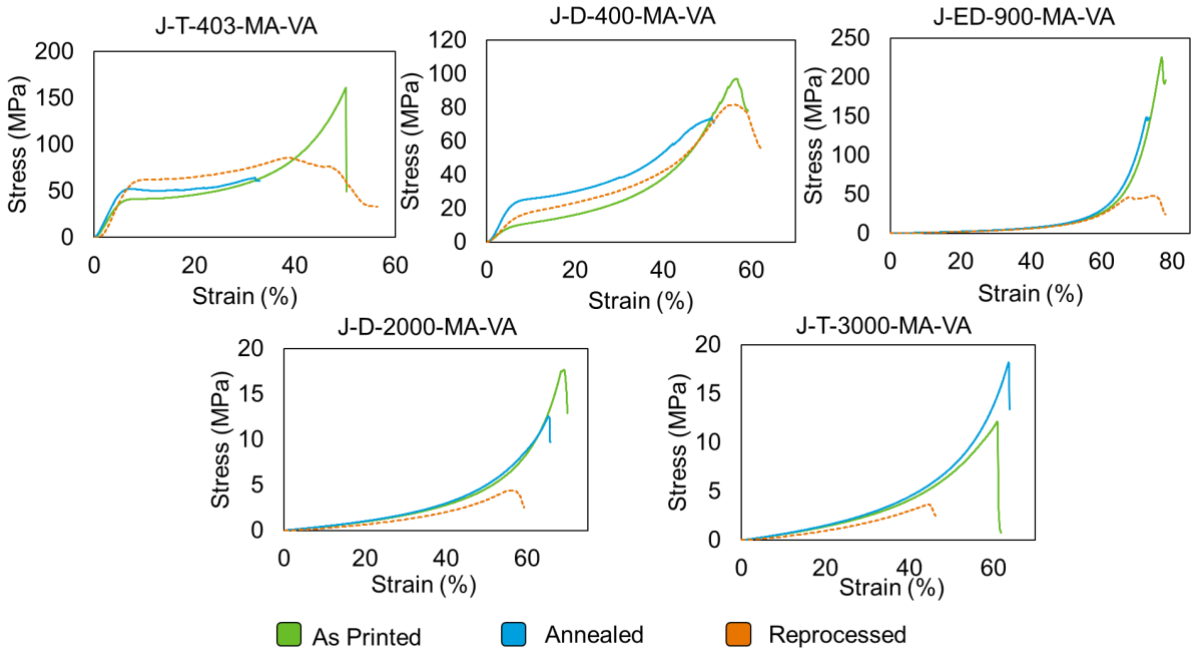

Figure S15. Comparison of mechanical properties in compression of as printed, annealed and reprocessed samples for the five different formulations.

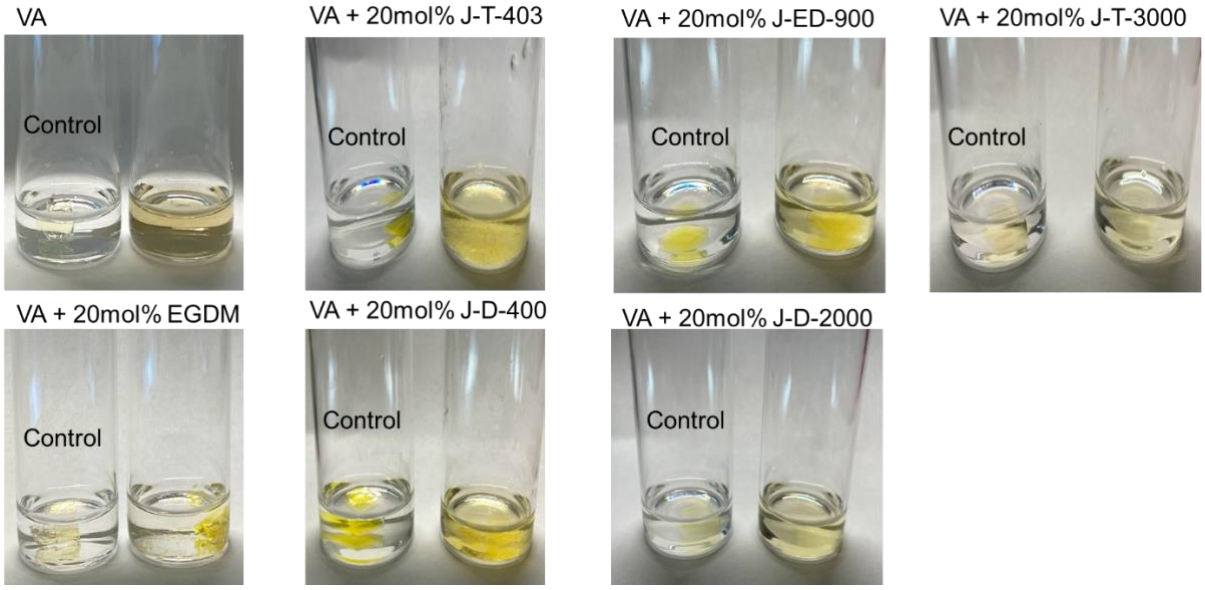

Figure S16. Chemical degradation experiments in 1M hexylamine/THF solution.

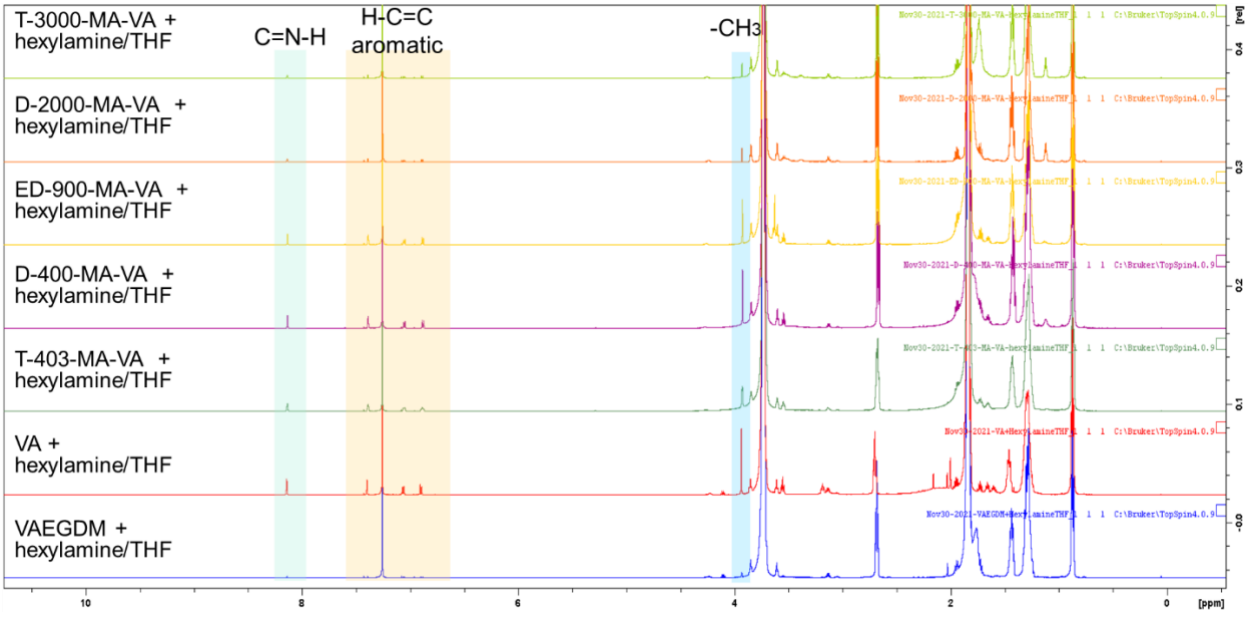

Figure S17. ^{1}H NMR spectra of the solution in 1M hexylamine/THF of the five polymers showing the characteristic peaks of vanillin.